Interfacial microstructure and mechanical behaviour in laser clad TiC_p/Ni alloy coatings

X. L. Wu and Y. S. Hong

Coatings of TiC_p reinforced composite have been produced by laser cladding. Two kinds of coating with different TiC_p origins were investigated, i.e. undissolved TiC_p and *in situ* TiC_p. For undissolved TiC_p, epitaxial growth of TiC, precipitation of CrB, and a chemical reaction occur at phase interfaces, and nanoindentation loading curves show pop in marks caused by the plastic deformation associated with crack formation or debonding of TiC_p from the matrix. As for *in situ* TiC_p, no pop in mark appears. Meanwhile, *in situ* TiC_p produces hardness and elastic modulus values that are higher than those produced by the coating that contains undissolved TiC_p. **MST/4637**

At the time this work was carried out the authors were in the State Key Laboratory of Non-linear Mechanics, Institute of Mechanics, Chinese Academy of Sciences, Beijing 100080, China. Dr Wu is now in the Chemical Engineering Department, Cleveland State University, 1960 East 24th Street, SH 455 Cleveland, OH 44115–2425, USA (wuxl_cas@hotmail.com).
Manuscript received 3 March 2000; accepted 22 August 2000.
© 2001 IoM Communications Ltd.

Introduction

Laser surface cladding can produce composite coatings for enhancing the wear, oxidation, and erosion resistances of material surfaces.[1,2] Abboud and West[3–5] produced functionally graded Fe–Al and Ni–Al coatings in the form of up to three superimposed clad layers of ~4 mm total thickness. By successive deposition of clad layers normal to the nickel and iron substrate surface the oxidation and erosion resistances were improved. Abbas and West[6] investigated a composite coating of SiC powder plus Stellite (CoNiWFeSiC) on EN3b steel. The hardness and wear resistances of the composite became more enhanced as the percentage of SiC particles was increased. Matthews[7] clad a Hastellite (50 WC and 50NiCrSiB) coating on a steel substrate and suggested that such a hard facing technique was highly promising for many applications. (All compositions given in this paper are in wt-% unless stated otherwise.) Lei *et al.*[8] analysed the microstructural characteristics of a 30TiC_p reinforced Ni alloy coating and found that the coating enhanced the abrasive wear resistance. Ayers and co-workers[9] injected 30–50 vol.-% of 100 μm TiC_p into the laser melted zone of a titanium alloy (Ti–6A–l4V) and observed an increase in the hardness to ~450 HV (0.4 N) and a decrease in the friction coefficient.

The microstructural characteristics and mechanical behaviour of the interfaces between the reinforcing particles and binder alloy are crucial to the overall properties of a coating. This is because the strengthening of the coating is caused by a transfer of stress that occurs at the interfaces through a shear mechanism. The interfacial structure of a reinforced particle can change to a high degree. As far as carbides are concerned, such as WC, SiC, and TiC, etc. dissolution to various degrees occurs when particles are in the laser generated molten pool, and subsequently, regrowth can occur during cooling. The chemical reaction between the particle and the binder metal often occurs at the phase interface. The reaction product has a strong influence upon the interfacial combination and bulk property of the coating. However, few microstructural observations and mechanical property determinations at phase interfaces have been reported.

Nanoindentation methods can be used to reliably study properties of interface regions in materials.[10] The scale of the deformation is small; depths and forces are in the range of a few nm and nN respectively. The 'nanomethod' exclusively adopts the contact compliance method. Direct imaging of the indent, while possible, is generally not a viable experimental procedure. The present work is a study of the microstructure and mechanical behaviours, such as hardness and elastic modulus, of phase interfaces between the reinforcing particle and the matrix.

Experimental

A commercial 5CrMnMo steel of composition Fe–0·43C–1·23Cr–1·18Mn–0·23Mo was used as the substrate. A powder mixture of 30 vol.-%TiC and 70 vol.-%Ni base alloy was used as the coating material. The chemical composition of the Ni alloy was Ni–16Cr–3·5B–4·5Si–0·8C. The Ni alloy particles had an average size of 40 μm and appeared to be spherical, while the TiC_p particles were <6 μm in size and irregular in shape. In order to obtain a pasty mixture TiC_p and polyethylene glycol were used. The paste was precoated onto the specimen surface to a thickness of ~0·8 mm by brushing.

A 3 kW cw CO_2 laser was used to produce the coating. The processing conditions were as follows: the scanning speed was 14 mm s^{-1}, the beam diameter was 3 mm, and the laser power was 2·5 kW. An argon atmosphere was used to shroud the molten pool from the surrounding air.

Another kind of TiC_p reinforced coating was obtained using the procedure described in Ref. 11. The coating material consisted of a powder mixture of titanium plus graphite (total 30 vol.-%) and a Ni alloy (70 vol.-%). The ratio of Ti to C powders corresponded to that of stoichiometric TiC. The average size and purity of the titanium and graphite powders were 8–12 μm and 20–40 μm, and 99·9 and 99·99 vol.-%, respectively. The laser processing parameters were power 2 kW, scanning speed 15 mm s^{-1}, and beam diameter 3 mm. Using this method, TiC_p was introduced into the coating by *in situ* reaction between the titanium and graphite.[11,12] The *in situ* TiC_p was different from the undissolved TiC_p in two respects. First, the size of *in situ* TiC_p was much smaller than that of undissolved TiC_p. Second, *in situ* TiC_p was compatible with the matrix and the phase interfaces were free from deleterious precipitation and chemical reactions.[11,12]

The morphology, microstructure, and interface structure of the coating were observed using SEM, TEM, and high

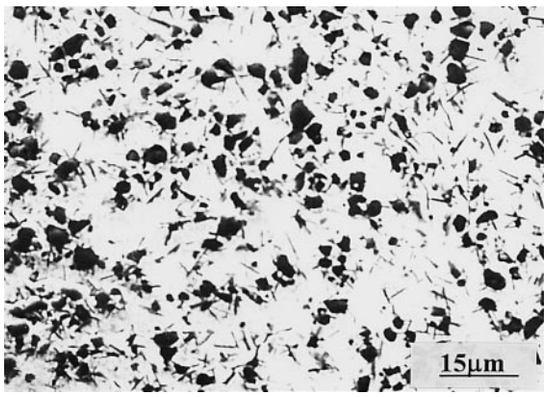

1 Micrographs showing coating reinforced by undissolved TiC_p (SEM)

resolution TEM (HRTEM) equipped with an electron energy loss spectrum (EELS).

The mechanical behaviours were studied in the matrix region near the phase interface between TiC_p and the matrix using a nanoindenter from the Swiss Centre for Electronics and Microtechnology. The load and displacement resolution was 0·3 μN and 0·17 nm respectively. A berkovich indenter was used and the indent location was controlled automatically by a computer. This instrument could monitor and record the dynamic load and displacement during indentation. The largest size of the indent region was about twice as large as the indent depth. Hardness H and elastic modulus E were calculated from the load *v.* displacement data obtained during nanoindentation. The hardness was calculated as the nominal stress underneath the indenter at any point in time, i.e. the load currently applied to the indenter divided by the current projected area. Since the indenter geometry was known, the area was, in practice, calculated directly from measurements of the total depth. The elastic contribution to this depth was subtracted so that the resulting hardness measurement could reflect the resistance of the material to plastic flow only. The relevant equations for calculating the modulus calculation are

$$\frac{1-v_i^2}{E_i} = \frac{1}{E_r} - \frac{1-v_s^2}{E_s} \quad \ldots\ldots\ldots\ldots (1)$$

and

$$E_r = \frac{1}{2h_p}\left(\frac{\pi}{\beta}\right)^{1/2}\left(\frac{dP}{dL}\right) \quad \ldots\ldots\ldots\ldots (2)$$

where v is the Poisson's ratio, and i and s refer to the indenter and sample, respectively. The composite modulus E_r is obtained from the unloading slope (dP/dL) and requires the determination of the plastic depth at which unloading began h_p, and β is a constant. A value of $v_i = 0{\cdot}31$ was chosen, since this was the Poisson's ratio for the Ni alloy.

Experimental results and discussion

INTERFACIAL STRUCTURE OF UNDISSOLVED TiC_p

Figure 1 shows an SEM of a cross-section of the coating and shows undissolved TiC_p dispersed in the coating. Image analysis indicates there is ~23 vol.-%TiC_p, which is similar to the amount of TiC_p produced by *in situ* reaction.[11]

Figure 2*a* is a bright field TEM showing the interfacial features of undissolved TiC_p. Two precipitates can be seen with thin loop-like and granular appearances respectively.

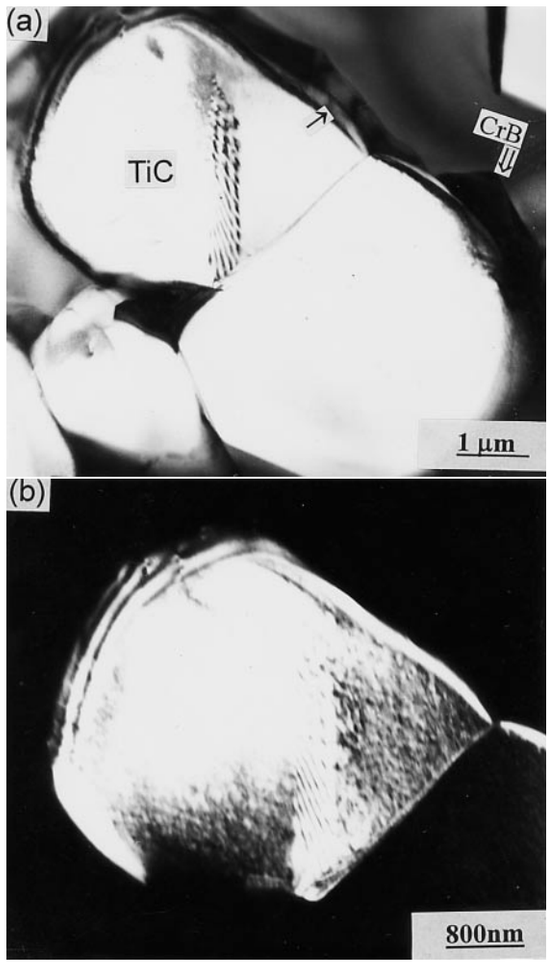

a bright field image showing ↑ epitaxial growth of TiC and ⇓ precipitation of CrB; *b* dark field

2 Micrographs of phase interface of undissolved TiC_p (TEM)

Figure 2*b* is a dark field TEM obtained using the diffraction spot (110) for TiC. It is deduced that the loop-like precipitate is grown epitaxially TiC. This is evidence of the partial dissolution of TiC_p during heating and regrowth during cooling. The granular precipitate is determined to be CrB by using selected area diffraction patterns. Nucleation of CrB at interfaces between TiC_p and the matrix is widely observed.

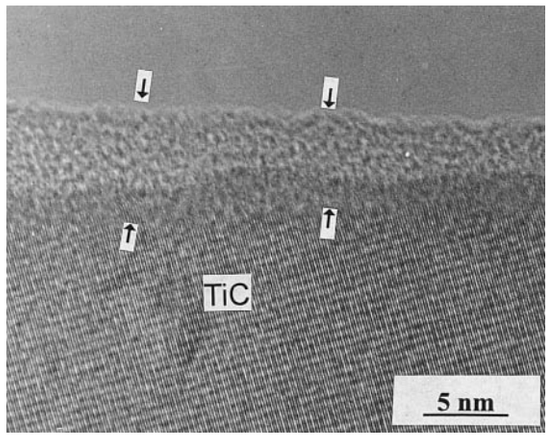

3 High resolution TEM showing chemical reaction layer around undissolved TiC_p

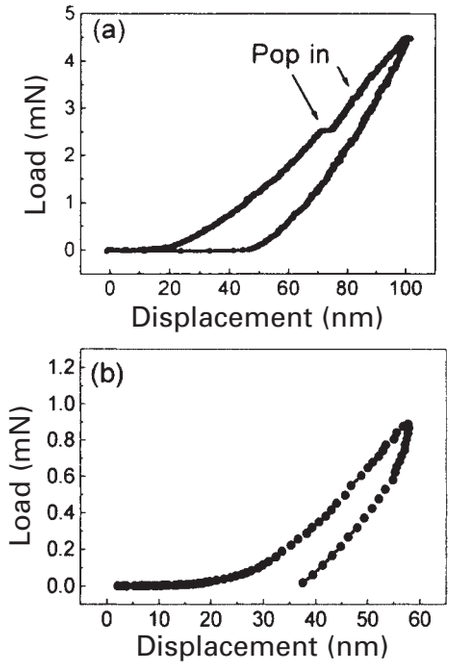

a undissolved TiC_p; *b in situ* TiC_p

4 Load–displacement curves near TiC_p interface: pop in marks indicated

Figure 3 shows an HRTEM of the interface of undissolved TiC_p. A thin reaction layer at the TiC_p edge is seen. The crystal structure has not been determined because of the small size of the layer. However, using EELS, the chemical composition of the layer is determined to consist of Ti and B. The content of B is in the range 38–63 at.-%. Thus, the formation of the layer is caused by the reaction of TiC_p with B in the matrix.

Therefore, epitaxial growth, a chemical reaction, and the formation of CrB occur at the interfaces of undissolved TiC_p. The microstructures and interface structures of *in situ* TiC_p have been studied in detail in Ref. 11. Contrary to undissolved TiC_p, the phase interface of *in situ* TiC_p is clean and free from precipitation or deleterious surface reactions.[11]

DISTRIBUTION OF HARDNESS AND MODULUS

Figure 4 shows representative load–displacement curves from the matrix region very near the interface between TiC_p and the matrix. Figure 4*a* and *b* corresponds to undissolved TiC_p and *in situ* TiC_p respectively. The nearest distance between the indent and the interface is ~200 and 120 nm for the undissolved and *in situ* TiC_p, respectively. Figure 4*a* shows several pop in marks, with displacements of between a few to tens of nanometres, from the beginning of loading and even with a very low load. It is further observed that for undissolved TiC_p, pop in marks occur universally in the loading curve with various loads. However, no pop in marks appear in Fig. 4*b* corresponding to *in situ* TiC_p.

Figure 5 reveals the distribution of E and H at matrix regions near phase interfaces with undissolved TiC_p and *in situ* TiC_p. The values of E and H have a gradient distributions. However, *in situ* TiC_p produces values of E and H that are much higher than does undissolved TiC_p.

Pop in marks in the loading curve reflect either the onset of plastic deformation associated with crack formation or the debonding of TiC_p from the matrix. A pop in mark can be considered as a token of the fracture toughness, i.e. the number of pop marks gives some idea of the resistance to

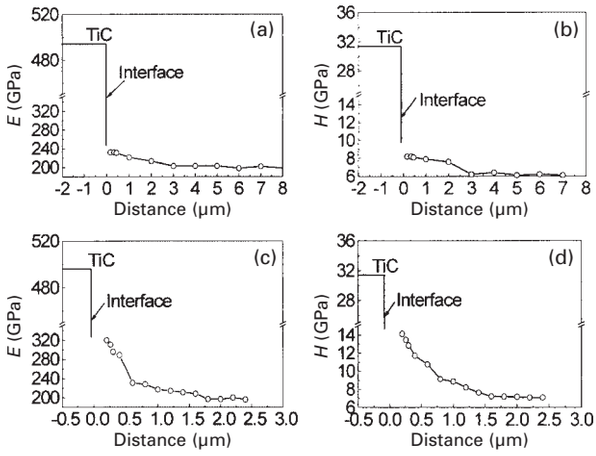

a,b undissolved TiC_p; *c,d in situ* TiC_p

5 Distribution of modulus and hardness near phase interface

crack initiation and propagation. Thus, the formation of a pop in mark may result from a low fracture toughness and has a close relationship with the interfacial microstructural features. The formation of brittle compounds owing to precipitation and chemical reaction at interfaces severely reduces the fracture toughness and leads to a low fracture stress. Therefore, the phase interface region of the undissolved TiC_p has a lower fracture toughness than that of *in situ* TiC_p.

In situ TiC_p is introduced into the matrix by a direct reaction and, as a result, the particle is more compatible with the matrix and the phase interface remains clean and free from a deleterious phase produced by an interface reaction.[11] This is considered to be one of the main advantages of interfaces generated *in situ*. Contrarily, precipitation of CrB and the formation of a chemical reaction layer occur around the phase boundaries of the undissolved TiC_p. Both the brittle intermetallic CrB and the chemical reaction layer injure the interface bond. Meanwhile, in the two kinds of composite coating with similar volume fractions of the reinforcing phase, the size of *in situ* TiC_p is finer than that of undissolved TiC_p. The strengthening effect of the reinforcing phase will increase as the particle size decreases. Therefore, *in situ* TiC_p may effectively enhance the hardness and modulus of the matrix, and relax the stress concentration at the phase interface.

Conclusions

1. Epitaxial growth of TiC, the formation of CrB, and a chemical reaction layer are observed at phase interfaces of undissolved TiC_p.
2. For undissolved TiC_p, the load–displacement curve shows pop in phenomena caused by the onset of plastic deformation associated with crack formation or the debonding of particles from the matrix. The generation of TiC_p *in situ* produces a higher toughness, hardness, and elastic modulus than does undissolved TiC_p.

Acknowledgements

This research was supported by the National Natural Science Foundation of China (Grant no. 19891180), the National Outstanding Youth Scientific Award of China

(Grant no. 19525205), and the Chinese Academy of Sciences.

References

1. W. M. STEEN: in ' Laser processing: surface treatment and thin film deposition', (ed. J. Mazumder *et al.*), 307; 1996, Dordrecht, Kluwer.
2. R. VILAR: *Mater. Sci. Forum*, 1999, **301**, 229.
3. J. H. ABBOUD and D. R. F. WEST: *Mater. Sci. Technol.*, 1991, **7**, 353.
4. J. H. ABBOUD and D. R. F. WEST: *J. Mater. Sci. Lett.*, 1992, **11**, 1675.
5. J. H. ABBOUD, D. R. F. WEST, and R. D. RAWLINGS: *Mater. Sci. Technol.*, 1994, **10**, 848.
6. G. ABBAS and D. R. F. WEST: *Wear*, 1991, **143**, 353.
7. S. J. MATTHEWS: in 'Applications of lasers in materials processing', (ed. E. A. Metzbower and S. M. Copler), 138; 1983, Materials Park, OH, American Society for Metals.
8. T. C. LEI, J. H. OUYANG, Y. T. PEI, and Y. ZHOU: *Mater. Sci. Technol.*, 1995, **11**, 520.
9. J. D. AYERS, T. R. TUOKER, and R. C. BOWERS: *Scr. Metall.*, 1980, **14**, 549.
10. W. C. OLIVER and G. M. PHARR: *J. Mater. Res.*, 1992, **7**, 1564.
11. X. L. WU: *Surf. Coat. Technol.*, 1999, **115**, 111.
12. X. L. WU: *J. Mater. Res.*, 1999, **14**, 2704.